

Wireless Network Localization via Alternating Projections with TDOA and FDOA Measurements

XIANGPING ZHAI^{1,*}, JUNJIE YANG² AND LIN CUI³

¹*College of Computer and Technology, Nanjing University of Aeronautics and Astronautics, China
Collaborative Innovation Center of Novel Software Technology and Industrialization, China*

²*College of Electronic and Information Engineering, Shanghai University of Electric Power, China*

³*Department of Computer Science, Jinan University, China*

Received: September 1, 2015. Accepted: January 25, 2017.

Localization is particularly important in wireless networks. With the rapid development of the Internet of Things and mobile Internet, mobility is becoming an increasingly growing topic. In this paper, we consider wireless network localization with the time difference of arrival (TDOA) and the frequency difference of arrival (FDOA) measurements which represent the mobility. To solve the maximum likelihood problem with the constraints that are imposed due to both TDOA and FDOA measurements, we adopt the alternating projection onto convex sets for source localization in sensor networks. Leveraging the convex approximation, we propose a convex boundary projection algorithm to estimate the source location. Numerical simulations show that our method is more efficient in distributed manner and the result is close to the Cramer-Rao lower bound performance under noisy measurements.

Keywords: Localization, wireless networks, alternating projection, time difference of arrival (TDOA), frequency difference of arrival (FDOA).

1 INTRODUCTION

Localization is a central concept in wireless sensor networks for many applications [18, 22, 27, 31]. Generally, this problem consists of two parts, i.e.,

* Contact author: E-mail: blueicezhaixp@nuaa.edu.cn

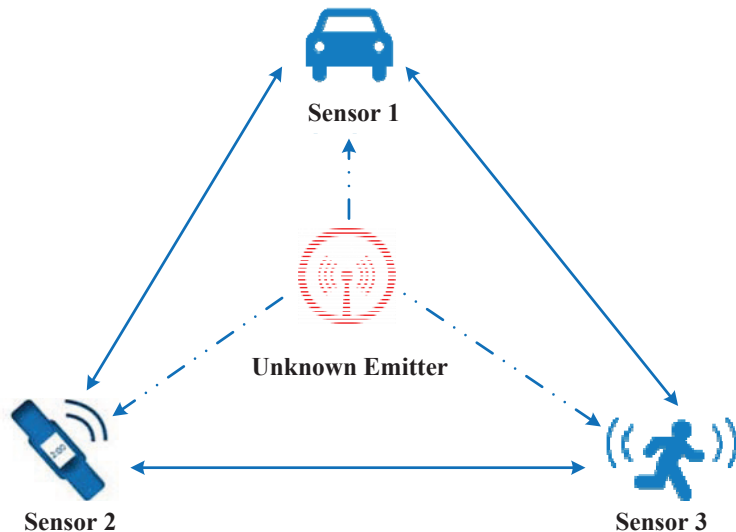


FIGURE 1

An illustration of the wireless network localization. The solid lines denote the information sharing between the sensor nodes. The dashed lines denote the measurements for the unknown emitter.

the localizability problem that checks for the feasibility of all distance measurement specification constraints and the localization problem that finds the locations of unknown emitter node given the feasible constraints. In this paper, we study the localization problem with one emitter node and many sensor nodes under the constraints that the emitter can be located. The measurements for localization usually use either the time of arrival (TOA), the time difference of arrival (TDOA), the angle of arrival (AOA) information or a combination of these techniques. When the emitter or the sensor nodes are moving, it is also practical to consider the localization technique that makes use of the frequency difference of arrival (FDOA) measurements in wireless networks, as illustrated in Figure 1.

There are three main well-studied methods to solve the localization problem for wireless sensor network when there are only TOA or TDOA measurements: 1) *Multidimensional scaling method* [4, 6, 9, 15, 26] is an optimal algorithm when there are no measurement noise and there are accurate distance measurement between all the nodes (transmitter-receiver pairs) in the networks. 2) *Convex optimization method* relaxes the nonconvex quadratic programming problem and provides good estimation performance by the computationally efficient suboptimal algorithm even in the presence of measurement noise. The localization problem is relaxed into either a convex second-order

cone program [21], or a semidefinite program [1, 12, 13, 19]. 3) *Alternating projection method* solves the localization problem by iteratively projecting onto the measurement constraints. In [2, 7], the authors show that the optimal estimation lies at the intersections of TOA constraints when the position of the unknown emitter is in the convex hull of the measurement constraints. In [16], the authors study the hyperbolic projection onto convex sets that tackles the situation when the position of unknown emitter lies outside of the convex hull of the measurement constraints. In [10, 24], this projection method is improved through the boundary projection configurations.

Recently, mobile characteristic has been an important issue as the developing Internet of Things has gradually included the wearable smart devices, vehicles and so on. In [3], the authors propose a novel method for the localization problem by only using a single sensor with the additional requirement that it is moving. In [11], the authors present a localization technique that uses the Doppler shift in radio transmission frequency for tracking and navigation in mobile wireless sensor networks. Therefore, the problem of localization via both TDOA and FDOA measurements has received significant attention due to its many applications in the mobile setting. In [14], the authors propose a robust and secure scheme for mobile node localization in the presence of malicious anchors. In practice, TDOA measurement is readily obtained through signal correlation at different receivers and this is useful for locating high-bandwidth emitter. On the other hand, FDOA measurement makes use of the difference in received Doppler frequency shift that is more useful for locating low-bandwidth emitter. TDOA and FDOA observation criteria are discussed in [5]. In [30], the authors consider the problem of joint TDOA and FDOA estimation for passive emitter location when the unknown emitter signal has a chirp-like structure over the observation interval. The Cramer-Rao lower bound (CRLB) on the TDOA and FDOA measurement errors is frequently so small that the errors induced by equipments are predominant. Therefore, the estimation is more accurate by leveraging a wider spectrum of bandwidth that combines both TDOA and FDOA measurements. However, different from TDOA measurement, the FDOA measurement makes the problem more challenging [8], because of the nonlinearity and nonconvexity. Researchers have applied the multidimensional scaling method [25] and the semidefinite relaxation method [23, 28] to the localization problem with FDOA measurements. On the other hand, the alternating projection method has not yet been studied to tackle the nonconvex FDOA measurement constraint that depends on the velocity of the nodes.

In this paper, we first show that the maximum likelihood estimation of the localization problem with both TDOA and FDOA measurements is equivalent to a convex feasibility problem. Then, we propose an alternating projection method through iteratively convexifying the FDOA constraint function

to obtain an approximated location of the unknown emitter. To the best of our knowledge, this is the first application of boundary projection algorithm in the localization problem with FDOA measurements. We also consider the local iterative optimization to improve the solution further by using the initial point obtained from the alternating projection. Numerical evaluation shows that the performance of our method achieve closely to the CRLB.

Overall, the contributions in this paper are:

1. a novel method by iteratively convexifying the FDOA measurement constraint function in a distributed manner,
2. the design of alternating projection algorithm for localization with both TDOA and FDOA measurements,
3. finding an efficient approximation of the location in the first stage to achieve the CRLB performance.

The rest of paper is organized as follows: In Section 2, we introduce the system model with TDOA and FDOA measurements, formulate the localization problem and provide the theoretical CRLB analysis. In Section 3, we consider the localization problem as a convex feasibility problem and propose a random alternating projection algorithm to obtain the location of the unknown emitter with accurate measurements. In Section 4, we modify our algorithm as weighted alternating projection algorithm to get the location of unknown emitter when there are Gaussian noise perturbations in the measurements. In Section 5, we compare our methods with the efficient convex relaxation method [28] and show that our method achieves the CRLB performance. In Section 6, we conclude the paper and consider future extensions.

The following notations are used in this paper: Boldface lowercase letters denote column vectors and italics denote scalars. The super-script $(\cdot)^T$ denotes the transpose. Let $|\cdot|$ denote the absolute value and $\|\cdot\|_2$ denote the Euclidean norm.

2 SYSTEM MODEL AND LOCALIZATION PROBLEM

In this section, we consider a cluster of passive receivers that collaborate to locate an unknown (and slowly moving) source emitter, while the orbits of the receivers are assumed to be known. We focus on two practical sensor measurements, i.e., TDOA and FDOA, in the network. Then, we formulate the localization problem. Without loss of generality and for illustration purpose, we assume that the vectors lie on \mathbb{R}^2 , but our method can be readily generalized to a higher dimension space.

2.1 Time Difference of Arrival

Let us define the i -th receiver node location as \mathbf{s}_i and the unknown emitter location as \mathbf{x} . The distance between the i -th receiver and the unknown emitter is given by:

$$d_i = \|\mathbf{x} - \mathbf{s}_i\|_2. \quad (1)$$

Let c denote the speed of light. Then, the TOA at the i -th receiver is given by:

$$t_i = \frac{\|\mathbf{x} - \mathbf{s}_i\|_2}{c}. \quad (2)$$

Measuring the time t_i , we get the distance $d_i = ct_i$. Then, the surface of (1) is a circle and it is well-known that three TOA measurements are sufficient to obtain the location of unknown emitter.

However, an accurate TOA measurement requires accurate synchronization of measurement time between the unknown source emitter and the receivers. Thus, in practice, the TDOA is used instead especially in mobile setting when the time synchronization of the unknown emitter cannot be achieved. The TDOA between receivers i and j is given as:

$$t_{ij} = t_i - t_j = \frac{\|\mathbf{x} - \mathbf{s}_i\|_2}{c} - \frac{\|\mathbf{x} - \mathbf{s}_j\|_2}{c}. \quad (3)$$

Let us rewrite (3) as the equivalent difference between distance:

$$d_{ij} = d_i - d_j = \|\mathbf{x} - \mathbf{s}_i\|_2 - \|\mathbf{x} - \mathbf{s}_j\|_2. \quad (4)$$

Then, the surface of (4) is one half of a hyperbolic that is constructed by measuring the difference of time t_{ij} . Figure 2 shows the curves of (1) and (4).

In this paper, we assume that the measurement t_{ij} is corrupted by zero-mean Gaussian noise power σ_t that leads to the measurement estimation error.

2.2 Frequency Difference of Arrival

Let us define the velocity of the i -th receiver as \mathbf{v}_i and the frequency of the signal from unknown emitter as f_0 . Then, the Doppler shift on the i -th receiver is given by:

$$f_i = \frac{(\mathbf{s}_i - \mathbf{x})^T \mathbf{v}_i}{c \|\mathbf{x} - \mathbf{s}_i\|_2} f_0. \quad (5)$$

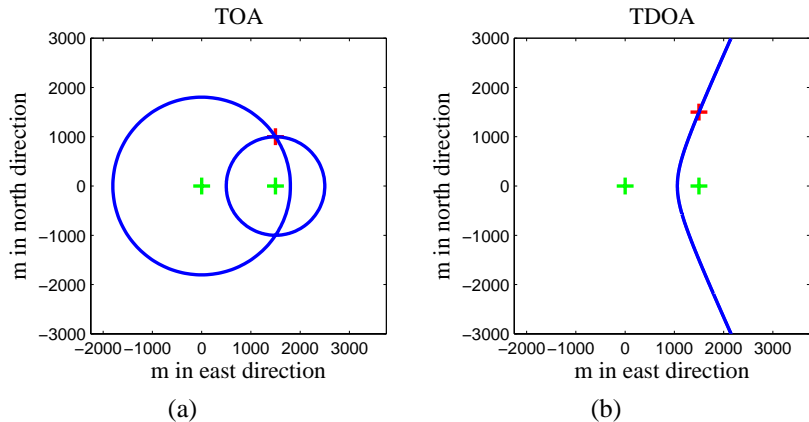


FIGURE 2

Illustrations for the curves of (a) TOA and (b) TDOA. The locations of receivers are $\mathbf{s}_1 = [0, 0]$ and $\mathbf{s}_2 = [1500, 0]$ m. The location of unknown emitter is $\mathbf{x} = [1500, 1000]$ m.

The angular form of the velocity expression is given by:

$$\mathbf{v}_i = \|\mathbf{v}_i\|_2 \begin{bmatrix} \cos \beta_i \\ \sin \beta_i \end{bmatrix}, \quad (6)$$

and the one of the distance is given by:

$$\mathbf{s}_i - \mathbf{x} = \|\mathbf{s}_i - \mathbf{x}\|_2 \begin{bmatrix} \cos \alpha_i \\ \sin \alpha_i \end{bmatrix}, \quad (7)$$

where α and β are the corresponding vector angles in the angular form for the distance and velocity, respectively. We then rewrite (5) as:

$$\alpha_i = \beta_i \pm \arccos \frac{cf_i}{\|\mathbf{v}_i\|_2 f_0}. \quad (8)$$

Therefore, the surface of (8) is viewed as the intersection of two rays. Compared to the Doppler shift measurement, FDOA measurement is preferred in practice due to its robustness feature. Therefore we consider the FDOA measurement given by:

$$f_{ij} = f_i - f_j = \frac{(\mathbf{s}_i - \mathbf{x})^T \mathbf{v}_i}{c\|\mathbf{x} - \mathbf{s}_i\|_2} f_0 - \frac{(\mathbf{s}_j - \mathbf{x})^T \mathbf{v}_j}{c\|\mathbf{x} - \mathbf{s}_j\|_2} f_0. \quad (9)$$

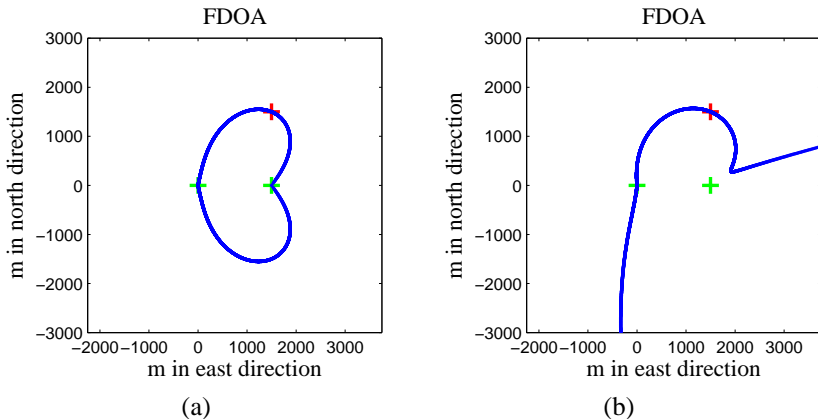


FIGURE 3

Illustrations for the different curves of FDOA. The locations of receivers are $\mathbf{s}_1 = [0, 0]$ m and $\mathbf{s}_2 = [1500, 0]$ m. The location of unknown emitter is $\mathbf{x} = [1500, 1500]$ m. (a) The receivers are moving in the same direction with velocities $\mathbf{v}_1 = [20, 0]$ m/s and $\mathbf{v}_2 = [10, 0]$ m/s. The corresponding difference of Doppler shift is $f_{21} = 14.14 f_0/c$. (b) The receivers are moving in the different direction with velocities $\mathbf{v}_1 = [20, 0]$ m/s and $\mathbf{v}_2 = [10, 6]$ m/s. The corresponding difference of Doppler shift is $f_{21} = 8.14 f_0/c$.

Different from the Doppler shift measurement that has a constant curve, (9) is a complicated nonlinear function that cannot be rewritten into the angular form straightforwardly. Figure 3 shows an example for the surface of the FDOA measurement that depends on the velocity of the receivers.

Note that we assume that the measurement f_{ij} is corrupted by zero mean Gaussian noise σ_f because of the observational error.

2.3 Localization Problem

Under both TDOA and FDOA measurement specification constraints, the unknown emitter source localization problem is formulated as the following maximum likelihood estimation problem:

$$\begin{aligned}
 & \text{minimize} && \frac{1}{\sigma_t^2} \sum_{i=1}^M \sum_{j>i}^M (t_i - t_j - t_{ij})^2 \\
 & && + \frac{1}{\sigma_f^2} \sum_{i=1}^M \sum_{j>i}^M (f_i - f_j - f_{ij})^2 \\
 & \text{subject to} && \frac{1}{c} \|\mathbf{x} - \mathbf{s}_i\|_2 = t_i, \quad \forall i, \\
 & && \frac{(\mathbf{s}_i - \mathbf{x})^T \mathbf{v}_i}{c \|\mathbf{x} - \mathbf{s}_i\|_2} f_0 = f_i, \quad \forall i, \\
 & \text{variables :} && \mathbf{x}, \mathbf{t}, \mathbf{f},
 \end{aligned} \tag{10}$$

where t_{ij} and f_{ij} are TDOA and FDOA measurements respectively [28] [29]. Now (10) is a nonlinear and nonconvex problem. As mentioned in the introduction, the multidimensional scaling method [25] and convex relaxation method [28] have been studied in the past to approximately solve (10). However, the computational complexity increases significantly with the number of receivers (or measurement constraints). Note that the maximum likelihood estimation (10) is equivalent to finding the set of node locations that minimizes the weighted squared-difference between the measured and the estimated internode distances. We propose our distributed method to solve this problem in the next section. To compare our localization method with the CRLB, we use the root-mean-square error defined as:

$$\text{RMSE} = \sqrt{\frac{1}{N} \sum_{n=1}^N \|\mathbf{x}(n) - \hat{\mathbf{x}}\|_2^2}, \quad (11)$$

where $\hat{\mathbf{x}}$ is the practical location of the unknown emitter, and $\mathbf{x}(n)$ is the n -th Monte-Carlo estimation of unknown emitter.

It is well known that the variance of an unbiased estimator is bounded below by the CRLB. The CRLB is used in this section to study the performance of the proposed location method. The CRLB is defined in terms of the sum of the Fisher information based on the TDOA and the FDOA measurements:

$$\mathbf{J} = \frac{1}{\sigma_t^2} \frac{\partial^2 \mathbf{t}}{\partial \mathbf{x} \partial \mathbf{x}^\top} + \frac{1}{\sigma_f^2} \frac{\partial^2 \mathbf{f}}{\partial \mathbf{x} \partial \mathbf{x}^\top}, \quad (12)$$

with entries of Jacobian of the TDOA measurement equations:

$$\frac{\partial t_{ij}}{\partial x_1} = \frac{x_1 - s_{i1}}{\|\mathbf{x} - \mathbf{s}_i\|_2} - \frac{x_1 - s_{j1}}{\|\mathbf{x} - \mathbf{s}_j\|_2}, \quad (13)$$

$$\frac{\partial t_{ij}}{\partial x_2} = \frac{x_2 - s_{i2}}{\|\mathbf{x} - \mathbf{s}_i\|_2} - \frac{x_2 - s_{j2}}{\|\mathbf{x} - \mathbf{s}_j\|_2}, \quad (14)$$

and the FDOA measurement equations:

$$\frac{\partial f_{ij}}{\partial x_1} = \frac{v_{j1} f_0}{c \|\mathbf{x} - \mathbf{s}_j\|_2} + \frac{(s_{j1} - x_1) v_{j1} x_1 f_0}{c \|\mathbf{x} - \mathbf{s}_j\|_2^3} - \frac{v_{j1} f_0}{c \|\mathbf{x} - \mathbf{s}_i\|_2} - \frac{(s_{i1} - x_1) v_{j1} x_1 f_0}{c \|\mathbf{x} - \mathbf{s}_i\|_2^3}, \quad (15)$$

$$\frac{\partial f_{ij}}{\partial x_2} = \frac{v_{j2} f_0}{\|\mathbf{x} - \mathbf{s}_j\|_2} + \frac{(s_{j1} - x_2) v_{j2} x_2 f_0}{\|\mathbf{x} - \mathbf{s}_j\|_2^3} - \frac{v_{j2} f_0}{\|\mathbf{x} - \mathbf{s}_i\|_2} - \frac{(s_{i1} - x_2) v_{j2} x_2 f_0}{\|\mathbf{x} - \mathbf{s}_i\|_2^3}. \quad (16)$$

The CRLB depends not only on the sensor-emitter geometry but also on the measurement standard deviations. Hence, the CRLB for the variance of the emitter location estimate \mathbf{x} is taken as the inverse of the Fisher information matrix, i.e. $\text{diag}\{\mathbf{J}^{-1}\}$. The unbiased estimator which achieves this lower bound is efficient.

3 RANDOM ALTERNATING PROJECTION ALGORITHM

Under accurate TDOA and FDOA measurements, (10) have a unique solution of the practical source location. However, (10) is a nonlinear least squares that has multiple local optimal solution and saddle points [7] in general. In this section, we solve this localization problem as a convex feasibility problem.

Let us first assume that the measurements t_{ij} and f_{ij} are accurate, then we rewrite (10) as:

$$\begin{aligned}
 & \text{minimize} && \sum_{i=1}^M \sum_{j>i}^M (t_i - t_j - t_{ij})^2 + \sum_{i=1}^M \sum_{j>i}^M (f_i - f_j - f_{ij})^2 \\
 & \text{subject to} && \frac{1}{c} \|\mathbf{x} - \mathbf{s}_i\|_2 = t_i, \quad \forall i, \\
 & && \frac{(\mathbf{s}_i - \mathbf{x})^T \mathbf{v}_i}{c \|\mathbf{x} - \mathbf{s}_i\|_2} f_0 = f_i, \quad \forall i, \\
 & \text{variables :} && \mathbf{x}, \mathbf{t}, \mathbf{f}.
 \end{aligned} \tag{17}$$

As the measurements are accurate, it is readily seen that the optimal value of (17) is zero and the optimal solution \mathbf{x}^* of (17) satisfies the constraints:

$$\begin{cases} \frac{1}{c} \|\mathbf{x}^* - \mathbf{s}_i\|_2 = t_i, & \forall i, \\ \frac{(\mathbf{s}_i - \mathbf{x}^*)^T \mathbf{v}_i}{c \|\mathbf{x}^* - \mathbf{s}_i\|_2} f_0 = f_i, & \forall i. \end{cases} \tag{18}$$

Next, let us define the sets $\partial\mathcal{C}_{ij}$:

$$\partial\mathcal{C}_{ij} = \{\mathbf{y} \in \mathbb{R}^2 : \|\mathbf{y} - \mathbf{s}_i\|_2 - \|\mathbf{y} - \mathbf{s}_j\|_2 = ct_{ij}\}, \tag{19}$$

and $\partial\mathcal{D}_{ij}$:

$$\partial\mathcal{D}_{ij} = \left\{ \mathbf{y} \in \mathbb{R}^2 : \frac{(\mathbf{s}_i - \mathbf{y})^T \mathbf{v}_i}{\|\mathbf{y} - \mathbf{s}_i\|_2} - \frac{(\mathbf{s}_j - \mathbf{y})^T \mathbf{v}_j}{\|\mathbf{y} - \mathbf{s}_j\|_2} = \frac{cf_{ij}}{f_0} \right\}, \tag{20}$$

where ∂ denotes the boundary of a region or the surface of a curve. Clearly, the practical emitter location lies on the intersection of the sets $\partial\mathcal{C}$ and $\partial\mathcal{D}$ when the TDOA and FDOA measurements are assumed to be accurate without noise corruption. Then, solving the problem (17) is equivalent to finding the point satisfying:

$$\mathbf{x}^* \in \bigcap_{i=1}^M \bigcap_{j>i}^M \partial\mathcal{C}_{ij} \bigcap_{i=1}^M \bigcap_{j>i}^M \partial\mathcal{D}_{ij}. \quad (21)$$

Although $\partial\mathcal{C}_{ij}$ is regarded as the boundary of a convex set:

$$\mathcal{C}_{ij} = \{ \mathbf{y} \in \mathbb{R}^2 : \|\mathbf{y} - \mathbf{s}_i\|_2 - \|\mathbf{y} - \mathbf{s}_j\|_2 \geq ct_{ij} \}, \quad (22)$$

$\partial\mathcal{D}_{ij}$ is nonconvex as shown in Section 2.2. Supposed that we are provided with accurate TOA measurements t_i , the FDOA measurement constraint function becomes linear as following:

$$\partial\mathcal{D}_{ij} = \left\{ \mathbf{y} \in \mathbb{R}^2 : \frac{(\mathbf{s}_i - \mathbf{y})^T \mathbf{v}_i}{d_i} - \frac{(\mathbf{s}_j - \mathbf{y})^T \mathbf{v}_j}{d_j} = \frac{cf_{ij}}{f_0} \right\}, \quad (23)$$

where $d_i = ct_i = \|\mathbf{y} - \mathbf{s}_i\|_2$. Then, (21) can be solved through the alternating projection onto the boundaries of convex sets that converges to the practical source location. In general, the assumption of accurate TOA measurements is not true, thus we iteratively improve the position \mathbf{x} by running the projection method with random initial points. This is summarized in the following random alternating projection algorithm.

Remark 1. *If the additional knowledge about the closest receiver to the emitter source is provided, this receiver is used as the initial node for projection, and we then make use of \mathbf{x} at each subsequent iteration of the projection method to linearize the FDOA measurement constraint function. A random projection strategy is used to avoid sequential projection that may cause limit circles in certain cases.*

The convergence of alternating projection algorithm for convex feasibility problem has been studied in [16] [24]. Figure 4 shows an example with accurate measurements in \mathbb{R}^2 in which Algorithm 1 converges to the practical emitter source location. Observe that at each iteration of the projected point on the convex boundary in Figure 4 (a), each iteration yields an approximated location of the unknown emitter source in Figure 4 (b).

Algorithm 1 Random Alternating Projection Algorithm.**1. Initialization**

- Choose the random position as $\mathbf{x}(0)$.
- Set $k = 1$.

• Projection

- Randomly pick two sensor nodes \mathbf{s}_i and \mathbf{s}_j .
- Projection onto hyperbolic TDOA boundary:

$$\mathbf{x}_{\partial C_{ij}(k)}(k) = \mathcal{P}_{\partial C_{ij}(k)}(\mathbf{x}(k-1)) = \arg \min_{\mathbf{z} \in \partial C_{ij}(k)} \|\mathbf{x}(k-1) - \mathbf{z}\|_2. \quad (24)$$

- Projection onto linear FDOA boundary:

$$\mathbf{x}_{\partial \mathcal{D}_{ij}(k)}(k) = \mathcal{P}_{\partial \mathcal{D}_{ij}(k)}(\mathbf{x}(k-1)) = \arg \min_{\mathbf{z} \in \partial \mathcal{D}_{ij}(k)} \|\mathbf{x}(k-1) - \mathbf{z}\|_2, \quad (25)$$

where the FDOA function is convexified by $\mathbf{x}(k-1)$:

$$\partial \mathcal{D}_{ij}(k) = \left\{ \mathbf{y} \in \mathbb{R}^2 : \frac{(\mathbf{s}_i - \mathbf{y})^T \mathbf{v}_i}{\|\mathbf{x}(k-1) - \mathbf{s}_i\|_2} - \frac{(\mathbf{s}_j - \mathbf{y})^T \mathbf{v}_j}{\|\mathbf{x}(k-1) - \mathbf{s}_j\|_2} = \frac{cf_{ij}}{f_0} \right\}. \quad (26)$$

- Repeat random projection for every pair of sensors.

2. Estimation

- Estimate $\mathbf{x}(k)$ as:

$$\begin{aligned} \mathbf{x}(k) = & \frac{2}{M(M-1)} \sum_{i=1}^M \sum_{j>i}^M \mathbf{x}_{\partial C_{ij}(k)}(k) \\ & + \frac{2}{M(M-1)} \sum_{i=1}^M \sum_{j>i}^M \mathbf{x}_{\partial \mathcal{D}_{ij}(k)}(k). \end{aligned} \quad (27)$$

3. Stop Condition

- If $\|\mathbf{x}(k) - \mathbf{x}(k-1)\|_2 < \epsilon$, stop;
- Else, set $k = k + 1$ and go to Step 2.

4 WEIGHTED ALTERNATING PROJECTION ALGORITHM FOR NOISY MEASUREMENTS

In practice, both the TDOA and FDOA measurements are not accurate and are assumed to be corrupted by Gaussian noise. Therefore, we consider the localization problem as (10) instead of (17), assuming that the measurement

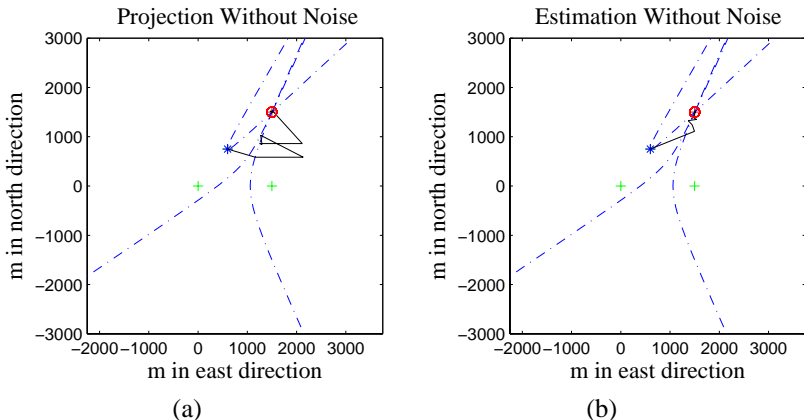


FIGURE 4

Convergence of Algorithm 1 under accurate measurements. The locations of receiver nodes are $\mathbf{s}_1 = [0, 0]$ m, $\mathbf{s}_2 = [1500, 0]$ m and $\mathbf{s}_3 = [600, 750]$ m. The location of unknown node is $\hat{\mathbf{x}} = [1500, 1500]$ m. The receivers are moving in the direction with velocities $\mathbf{v}_1 = [20, 0]$ m/s, $\mathbf{v}_2 = [20, 0]$ m/s and $\mathbf{v}_3 = [12, 12]$ m/s. (a) An illustration for each alternating projection. (b) An illustration for the estimation in each iteration.

noise in the TDOA and FDOA constraints are independent of each other. In this section, we improve Algorithm 1 to obtain an approximate solution to solve (10).

Due to the measurement noise, the intersection of sets $\partial\mathcal{C}$ and $\partial\mathcal{D}$ might be large or even be empty and, in such a case, the convergence has the characteristics to yield a point that minimizes the sum of distances to the sets $\partial\mathcal{C}_{ij}$ and $\partial\mathcal{D}_{ij}$, that is:

$$\mathbf{x}^* = \arg \min_{\mathbf{x} \in \mathbb{R}^2} \frac{1}{\sigma_t^2} \sum_{i=1}^M \sum_{j>i}^M \|\mathbf{x} - \mathcal{P}_{\partial\mathcal{C}_{ij}}(\mathbf{x})\|_2^2 + \frac{1}{\sigma_f^2} \sum_{i=1}^M \sum_{j>i}^M \|\mathbf{x} - \mathcal{P}_{\partial\mathcal{D}_{ij}}(\mathbf{x})\|_2^2. \quad (28)$$

Moreover, note that the distance measurement $d_{ij} = ct_{ij}$ should satisfy the triangle inequality $|d_{ij}| < \|\mathbf{s}_i - \mathbf{s}_j\|_2$. Otherwise, the TDOA function (4) is invalid on the hyperbolic surface. When the TDOA measurement estimates violate the triangle inequality condition, the corresponding measurement t_{ij} cannot be used. We improve Algorithm 1 to the following weighted alternating projection algorithm.

Remark 2. In Algorithm 2, we have used the noise power characteristic in the TDOA and FDOA measurements to minimize the weighted squared-differences between the estimated locations.

Algorithm 2 Weighted Alternating Projection Algorithm.

 Replace Step 3) in Algorithm 1 with:

- Estimate $\mathbf{x}(k)$ as:

$$\begin{aligned} \mathbf{x}(k) = & \frac{2\sigma_f^2}{M(M-1)(\sigma_t^2 + \sigma_f^2)} \sum_{i=1}^M \sum_{j>i}^M \mathbf{x}_{\partial C_{ij}}(k) \\ & + \frac{2\sigma_t^2}{M(M-1)(\sigma_t^2 + \sigma_f^2)} \sum_{i=1}^M \sum_{j>i}^M \mathbf{x}_{\partial D_{ij}}(k). \end{aligned} \quad (29)$$

As we have assumed random noise contaminating both the TDOA and FDOA measurements, the position estimates are in fact random variables. The position estimate at iteration k only depends on the previous position estimate, and the convergence in such a case has the characteristics of the position estimates approaching a neighborhood of \mathbf{x} and then “rattling around” [17]. By averaging the position estimates, the mean location position is an unbiased estimate as the measurement errors are assumed to be zero-mean random variables.

In the following, we give an illustration of the emitter source lying inside the convex hull of the measurement constraints given by:

$$\mathcal{H} = \left\{ \mathbf{y} \in \mathbb{R}^2 : \mathbf{y} = \sum_{l=1}^L \xi_l \mathbf{s}_l, \xi_l \geq 0, \sum_{l=1}^L \xi_l = 1 \right\}. \quad (30)$$

Figure 5 shows the unknown emitter lying inside the convex hull \mathcal{H} with Gaussian noise measurements in \mathbb{R}^2 . Similarly to Figure 4, each iteration denotes the projected point on the convex boundary in Figure 5 (a) and the estimated average location for the unknown emitter source in Figure 5 (b). Compared with the alternating projection algorithm that depends solely on the TOA or TDOA measurements, our algorithm has efficient performance when we also consider the FDOA measurement together with the TDOA measurement, and the location estimate is iteratively improved at each iteration.

The estimate position is also close to the practical position (i.e., the optimal solution of (10)) under noisy measurements. To get more accurate estimation, we can use the estimate position of Algorithm 2 as a starting point for a further local optimization.

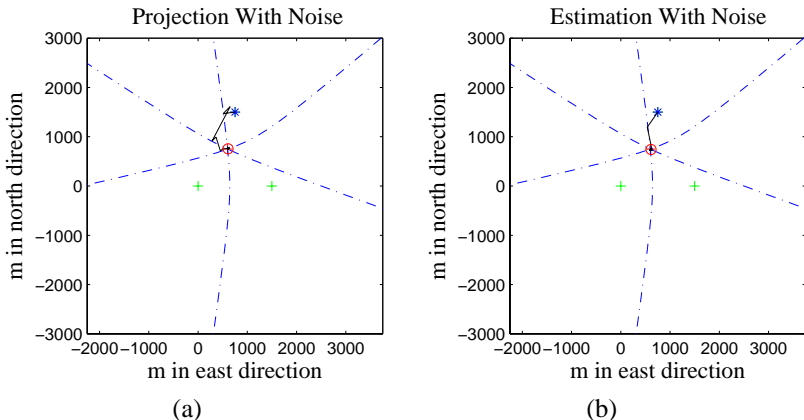


FIGURE 5

Convergence of Algorithm 2 under noisy measurements. The locations of receiver nodes are $\mathbf{s}_1 = [0, 0]$ m, $\mathbf{s}_2 = [1500, 0]$ m and $\mathbf{s}_3 = [750, 1500]$ m. The location of unknown emitter is $\hat{\mathbf{x}} = [600, 750]$ m. The receivers are moving in the direction with velocities $\mathbf{v}_1 = [20, 0]$ m/s, $\mathbf{v}_2 = [0, 20]$ m/s and $\mathbf{v}_3 = [-8, -8]$ m/s. The measurement of TDOA is the zero mean Gaussian $\sigma_t = 30$ ns. The measurement of FDOA is the zero mean Gaussian $\sigma_f = 0.1\sigma_t$. (a) An illustration for each alternating projection. (b) An illustration for the estimation in each iteration.

5 EXPERIMENTS

In this section, we compare our alternating projection algorithm with the known convex relaxation [28] and also the CRLB performance in estimation. Note that our proposed algorithm is more efficient in distribute manner while the convex relaxation is in centralized manner. We add the noise to the measurement in simulation, and run $N = 30$ times Monte-Carlo simulations for each different noise σ_t .

In practice, FDOA and TDOA measurements are taken as the peak arguments of Complex Ambiguity Function (CAF) of the emitter signals $s_1(\tau)$ and $s_2(\tau)$ which are received by the sensors. Efficient calculation of the CAF is presented in [20]:

$$A(t, f) = \int_0^T s_1(\tau)s_2(\tau + t)e^{-2\pi jf\tau} d\tau, \quad (31)$$

where T is the integration time, t is the difference of the arrival time, f is the difference of the Doppler shift, and $j = \sqrt{-1}$ denotes the imaginary unit. Then, the TDOA and FDOA measurements are the arguments of the maximum complex envelope of the CAF:

$$\{t, f\} = \arg_{t, f} \max A(t, f). \quad (32)$$

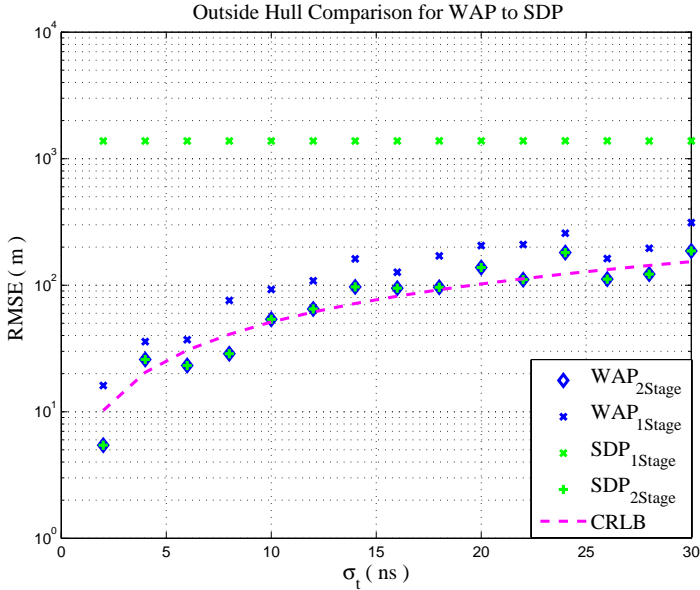


FIGURE 6

Comparison of the two stages estimation between weighted alternating projection algorithm and the semidefinite relaxation algorithms in [28] when $\sigma_f = 0.1\sigma_t$. The unknown node lies outside the convex hull, and the other parameters are the same as ones in Figure 4.

Example 1. We choose the location of unknown emitter as $\hat{\mathbf{x}} = [1500, 1500]$ m, which lies outside the convex hull of three receiver nodes. The receiver nodes are moving from the location of $\mathbf{s}_1 = [0, 0]$ m, $\mathbf{s}_2 = [1500, 0]$ m and $\mathbf{s}_3 = [600, 750]$ m to the direction denoted by the velocities $\mathbf{v}_1 = [20, 0]$ m/s, $\mathbf{v}_2 = [0, 20]$ m/s and $\mathbf{v}_3 = [12, 12]$ m/s.

In Figure 6, we compare our weighted alternating projection algorithm (denoted by WAP) to the two-pronged approach (denoted by SDP) in semidefinite relaxation [28]. For the convenience of comparison, we use the local optimization (Newton type method) to refine the approximated solution so as to obtain the better location estimation. Meanwhile, we use “1Stage” and “2Stage” to denote the estimation in the first and second stage for both algorithms, respectively. In addition, σ_t is the zero mean Gaussian for the noise measurement of TDOA, and $\sigma_f = n\sigma_t$ means that the FDOA measurement noise standard deviation is assumed n times that of TDOA in each Monte-Carlo simulations. It is observed that the final RMSEs of both WAP and SDP approach the CRLB curve. While the second stage of WAP is just the same superb as the one of SDP, the estimation in the first stage of WAP is far better than the one of SDP. In Figure 7, we compare our WAP algorithm

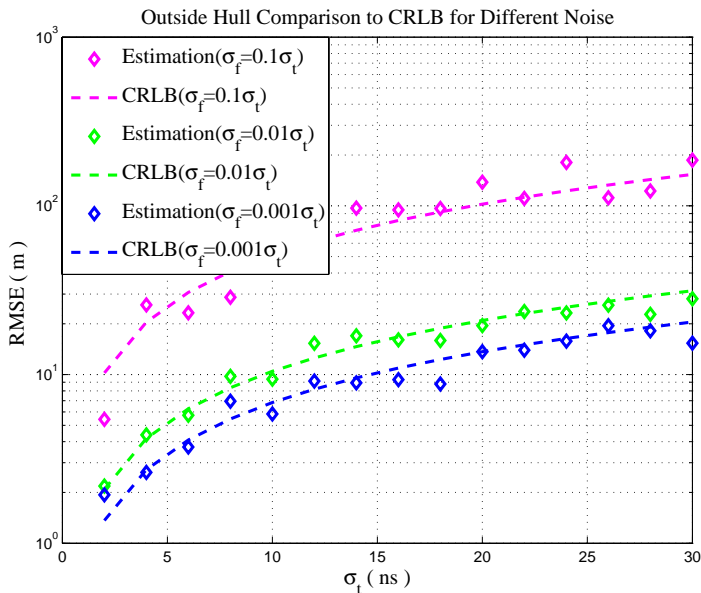


FIGURE 7

Comparison of the estimation in weighted alternating projection algorithm and the CRLB for the different relationship between σ_f and σ_τ . The unknown node lies outside the convex hull, and the other parameters are the same as ones in Figure 4.

for the different relationship between σ_f and σ_τ . The numerical evaluations show that the RMSE of the estimation is larger when the mean of the Gaussian noise distribution in the FDOA measurement σ_f is larger for the same σ_τ , and all of them achieve the CRLB.

Example 2. We choose the location of unknown emitter as $\hat{\mathbf{x}} = [600, 750]$ m, which lies inside the convex hull of three receiver nodes. The receiver nodes are moving from the locations of $\mathbf{s}_1 = [0, 0]$ m, $\mathbf{s}_2 = [1500, 0]$ m and $\mathbf{s}_3 = [750, 1500]$ m to the direction denoted by the velocities $\mathbf{v}_1 = [20, 0]$ m/s, $\mathbf{v}_2 = [0, 20]$ m/s and $\mathbf{v}_3 = [-8, -8]$ m/s.

In Figure 8, it is observed that the RMSEs of both WAP and SDP also approach the CRLB curve for the inside convex hull case. Moreover, the RMSE of the estimation increases almost linearly with the noise power. In Figure 9, the RMSEs of the estimation for the different relationship between σ_f and σ_τ are the same efficient with the outside convex hull case. We establish that our WAP approach runs in a distributed manner and improves the estimation in the first stage. In addition, the numerical evaluations show that the alternating projection algorithm converges relatively fast, as typically

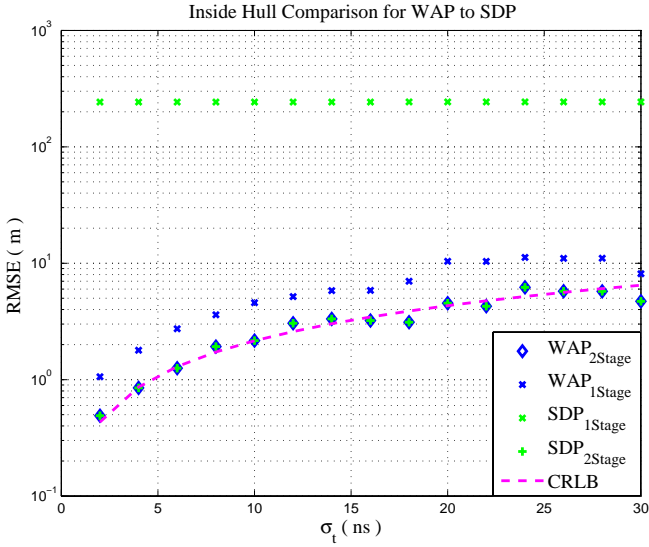


FIGURE 8 Comparison of the two stages estimation between weighted alternating projection algorithm and the semidefinite relaxation algorithms in [28] when $\sigma_f = 0.1\sigma_t$. The unknown node lies inside the convex hull, and the other parameters are the same as ones in Figure 5.

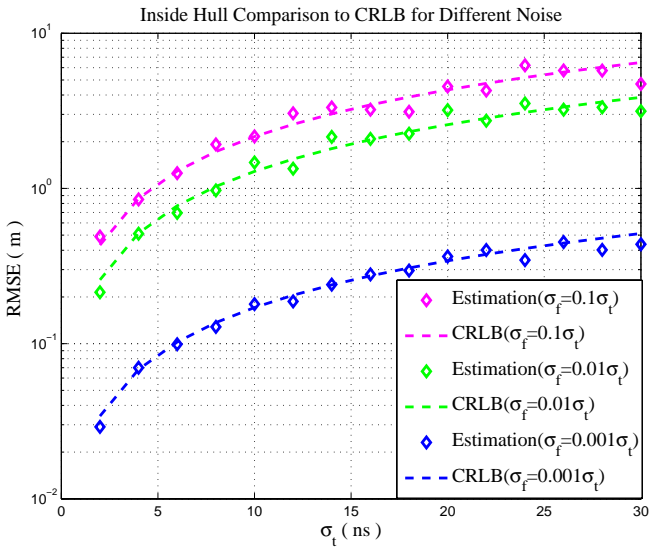


FIGURE 9 Comparison of the estimation in weighted alternating projection algorithm and the CRLB for the different relationship between σ_f and σ_t . The unknown node lies inside the convex hull, and the other parameters are the same as ones in Figure 5.

each simulation in our experiments requires less than 0.2s (on a desktop computer).

6 CONCLUSION

In this paper, we studied the problem of source localization with both TDOA and FDOA measurements in wireless networks. This nonconvex problem was converted into a convex feasibility problem by iterative convexifying of the FDOA measurement constraint function, and then was solved via a weighted alternating projection method. The alternating projection algorithm has efficient performance in the distributed manner of the first stage that the unknown node lies outside or inside the convex hull of the measurement constraints. Numerical experiments show that the iterative solution has the convergence properties that are close to the CRLB performance. For illustrative purpose, we have studied the two-dimensional case of localization, but the algorithm can be easily generalized to a higher dimension space (e.g., $\mathbf{x} \in \mathbb{R}^3$). Our approach has been based on the assumption that the source is stationary or slowly moving. We will track the dynamic target in the future work.

ACKNOWLEDGMENTS

The authors would like to thank the editors and reviewers who offered great help on improving this paper. The authors acknowledge helpful discussions with Prof. Chee Wei Tan, Prof. Gang Wang, Dr. Xiaojun Zhu and Mr. Lizhong Jiang. This work was jointly supported by the Natural Science Foundation of Jiangsu Province under Grant BK20140835, the Postdoctoral Foundation of Jiangsu Province under Grant 1401018B, the Fundamental Research Funds for the Central Universities under Grant NS2015094 and the National Natural Science Foundation of China under Grant 61402200.

REFERENCES

- [1] Biswas, P., Lian, T.-C., Wang, T.-C., and Ye, Y. (May 2006). Semidefinite programming based algorithms for sensor network localization. *ACM Transactions on Sensor Networks*, 2(2):188–220.
- [2] Blatt, D. and Hero, A. O. (Sept. 2006). Energy-based sensor network source localization via projection onto convex sets. *IEEE Transactions on Signal Processing*, 54(9):3614–3619.

- [3] Chen, X., Schonfeld, D., and Khokhar, A. A. (Oct. 2009). Localization and trajectory estimation of mobile objects using minimum samples. *IEEE Transactions on Vehicular Technology*, 58(8):4439–4446.
- [4] Chen, Z.-X., Wei, H.-W., Wan, Q., Ye, S.-F., and Yang, W.-L. (May 2009). A supplement to multidimensional scaling framework for mobile location: A unified view. *IEEE Transactions on Signal Processing*, 57(5):2030–2034.
- [5] Chestnut, P. C. (Mar. 1982). Emitter location accuracy using TDOA and differential doppler. *IEEE Transactions on Aerospace and Electronic Systems*, AES-18(2):214–218.
- [6] Costa, J. A., Patwari, N., and Hero, A. O. (Feb. 2006). Distributed weighted-multidimensional scaling for node localization in sensor networks. *ACM Transactions on Sensor Networks*, 2(1):39–64.
- [7] Hero, A. O. and Blatt, D. (Mar. 2005). Sensor network source localization via projection onto convex sets (POCS). *Proceedings of IEEE International Conference on Acoustics, Speech, and Signal Processing*, pages iii/689–iii/692.
- [8] Ho, K. C. and Chan, Y. T. (Jul. 1997). Geolocation of a known altitude object from TDOA and FDOA measurements. *IEEE Transactions on Aerospace and Electronic Systems*, 33(3):770–783.
- [9] Ji, X. and Zha, H. (2004). Sensor positioning in wireless ad-hoc sensor networks using multidimensional scaling. *IEEE INFOCOM*, 4:2652–2661.
- [10] Jia, T. and Buehrer, R. M. (Sept. 2011). A set-theoretic approach to collaborative position location for wireless networks. *IEEE Transactions on Mobile Computing*, 10(9):1264–1275.
- [11] Kusý, B., Amundson, I., Sallai, J., Völgyesi, P., Lédeczi, A., and Koutsoukos, X. (Aug. 2010). RF doppler shift-based mobile sensor tracking and navigation. *ACM Transaction on Sensor Networks*, 7(1):1–32.
- [12] Lui, K. W. K., Ma, W.-K., So, H. C., and Chan, F. K. W. (Feb. 2009). Semi-definite programming algorithms for sensor network node localization with uncertainties in anchor positions and/or propagation speed. *IEEE Transactions on Signal Processing*, 57(2):752–763.
- [13] Meng, C., Ding, Z., and Dasgupta, S. (2008). A semidefinite programming approach to source localization in wireless sensor networks. *IEEE Signal Processing Letters*, 15:253–256.
- [14] Misra, S., Xue, G., and Bhardwaj, S. (Mar. 2009). Secure and robust localization in a wireless ad hoc environment. *IEEE Transactions on Vehicular Technology*, 58(3):1480–1489.
- [15] Qin, S., Wan, Q., Chen, Z.-X., and Huang, A.-M. (Feb. 2011). Fast multidimensional scaling analysis for mobile positioning. *IET Signal Processing*, 5(1):81–84.
- [16] Rydstrom, M., Strom, E. G., and Svensson, A. (Jul. 2006). Robust sensor network positioning based on projection onto circular and hyperbolic convex sets (POCS). *IEEE Workshop on Signal Processing Advances in Wireless Communications*, pages 1–5.
- [17] Sethares, W. A. and Johnson, C. R. (Jan. 1989). A comparison of two quantized state adaptive algorithms. *IEEE Transactions on Acoustics, Speech and Signal Processing*, 37(1):138–143.
- [18] Shen, J., Tan, H., Wang, J., Wang, J., and Lee, S. (2015). A novel routing protocol providing good transmission reliability in underwater sensor networks. *Journal of Internet Technology*, 16(1):171–178.

- [19] Srirangarajan, S., Tewfik, A. H., and Luo, Z.-Q. (Dec. 2008). Distributed sensor network localization using SOCP relaxation. *IEEE Transactions on Wireless Communications*, 7(12):4886–4895.
- [20] Stein, S. (Jun. 1981). Algorithms for ambiguity function processing. *IEEE Transactions on Acoustics, Speech, and Signal Processing*, ASSP-29(3):588–599.
- [21] Tseng, P. (Feb. 2007). Second-order cone programming relaxation of sensor network localization. *SIAM Journal on Optimization*, 18(1):156–185.
- [22] Velimirovic, M., Djordjevic, G. L., Velimirovic, A. S., and Denic, D. B. (Nov. 2014). Range-free localization in wireless sensor networks using fuzzy logic. *Adhoc & Sensor Wireless Networks*, 23(3/4):187–210.
- [23] Wang, G., Li, Y., and Ansari, N. (Feb. 2013). A semidefinite relaxation method for source localization using TDOA and FDOA measurements. *IEEE Transactions on Vehicular Technology*, 62(2):853–862.
- [24] Wang, J. and Regalia, P. A. (Mar. 2009). Sensor network localization via boundary projections. *Conference on Information Sciences and Systems*, pages 224–229.
- [25] Wei, H.-W., Peng, R., Wan, Q., Chen, Z.-X., and Ye, S.-F. (Mar. 2010). Multidimensional scaling analysis for passive moving target localization with TDOA and FDOA measurements. *IEEE Transactions on Signal Processing*, 58(3):1677–1688.
- [26] Wei, H.-W., Wan, Q., Chen, Z.-X., and Ye, S.-F. (Jul. 2008). A novel weighted multidimensional scaling analysis for time-of-arrival-based mobile location. *IEEE Transactions on Signal Processing*, 56(7):3018–3022.
- [27] Wen, X., Shao, L., Xue, Y., and Fang, W. (2015). A rapid learning algorithm for vehicle classification. *Information Sciences*, 295(1):395–40.
- [28] Yang, K., Jiang, L., and Luo, Z.-Q. (May 2011). Efficient semidefinite relaxation for robust geolocation of unknown emitter by a satellite cluster using TDOA and FDOA measurements. *IEEE International Conference on Acoustics, Speech and Signal Processing*, pages 2584–2587.
- [29] Yang, K., Wang, G., and Luo, Z.-Q. (Jul. 2009). Efficient convex relaxation methods for robust target localization by a sensor network using time differences of arrivals. *IEEE Transactions on Signal Processing*, 57(7):2775–2784.
- [30] Yeredor, A. and Angel, E. (Apr. 2011). Joint TDOA and FDOA estimation: A conditional bound and its use for optimally weighted localization. *IEEE Transactions on Signal Processing*, 59(4):1612–1623.
- [31] Zhao, J., Mo, L., Wu, X., Wang, G., Liu, E., and Dai, D. (Nov. 2009). Error estimation of iterative maximum likelihood localization in wireless sensor networks. *Adhoc & Sensor Wireless Networks*, 23(3/4):277–295.